Asian Journal of Chemistry; Vol. 38, No. 2 (2026), 543-551
ASIAN JOURNAL OF CHEMISTRY
https://doi.org/10.14233/ajchem.2026.35106

Effect of Green Silver Nanoparticle Synthesised by *W. coagulans* on Carbapenamse Resistant Gene Down Regulation Antibacterial Efficacy

J. ISHWARYA and D. SANGEETHA*,

Department of Microbiology, Faculty of Science, Annamalai University, Chidambaram-608002, India

*Corresponding author: E-mail: ishumbjasmin@gmail.com

Received: *Accepted*: *Published online*: AJC-0000

The present study investigates the phytochemical profile, phylogenetic relationships and antibacterial activity of *Withania coagulans*, along with the green synthesis of silver nanoparticles (AgNPs) and their effects on cytotoxicity and the downregulation of pathogenicity-related genes. Phytochemicals were extracted using Soxhlet extraction and AgNPs were synthesized *via* a one-step green synthesis approach. The synthesized nanoparticles were characterized using UV-Visible, FTIR and TEM techniques. The antibacterial efficacy of AgNPs against imipenem-resistant pathogens was evaluated, followed by cytotoxicity assessment. The results revealed that methanolic and chloroform extracts were rich in bioactive phytochemicals, which likely contributed to the enhanced antibacterial activity and biocompatibility of the synthesized AgNPs. These extracts also showed notable antibacterial activity at 100 µg/mL, producing inhibition zones of 13-22 mm especially against *Klebsiella pneumoniae* and *Streptococcus pneumoniae*. UV-Visible spectrophotometry confirmed characteristic peak at 210-230 nm attributed by phytochemical reducing agents. Size of AgNP were 20 to 95 nm and spherical in nature. The biosynthesised AgNPs demonstrated strong antibacterial effects, with inhibition zones of 17-21 mm across all tested clinical isolates. The qPCR analysis further showed substantial down-regulation (70-95%) of resistance associated genes, with fold-change values ranging from 0.045 to 0.51, indicating potent transcriptional suppression. Cytotoxicity assessment on A549 cells showed mild toxicity, maintaining high viability (91.8-95%) up to 100 µg/mL with preserved cell morphology confirming the biocompatibility of the nanoparticles. The findings establish *W. coagulans* as a genetically authenticated and phytochemically rich source for biosynthesised AgNPs with significant antibacterial and gene inhibitory activities and limited cytotoxicity, supporting its potential for biomedical applications.

Keywords: *W. coagulans*, Phenol, Nanoparticle, RNA expression, Antibacterial activity, Carbapenem.

INTRODUCTION

Bacteria are subjected to environmental pressure when antibiotics are used inappropriately or improperly, which might result in mutations. These modifications improve the bacteria's stability and fitness, enabling them to thrive in antibiotic-containing environments. As a result, this condition encourages the emergence of multi-drug resistance (MDR), especially because carbapenem-resistant Enterobacteriaceae (CRE) are becoming more common [1,2]. NDM (bla_{NDM}, New Delhi metallo-β-lactamase) is one of the most common and extensive forms of carbapenemases, increasing the risk of bacterial infections in patients. In order to address antibiotic resistance, it is critical to find new potential therapeutic targets given the rise in NDM and the lack of novel antibiotics [3,4].

By altering membrane integrity and inhibiting efflux-pump mechanisms, producing reactive oxygen species (ROS) and inhibiting respiratory enzymes, biosynthesised AgNPs have been shown in recent work to significantly inhibit the growth of carbapenem-resistant pathogens highlighting their potential therapeutic value [5]. Due to their high surface-to-volume ratio and ability to interfere with carbapenemase-mediated resistance mechanisms, green-synthesized silver nanoparticles (AgNPs) exhibit significant potential as novel antibacterial agents [6]. Numerous plant species and their various parts, including leaves, fruits, vegetables, oilseeds, herbs, bark and roots, have been extensively explored as sources of phyto-chemicals that act as eco-friendly reducing and capping agents during nanoparticle synthesis. In this context, medicinal plants rich in antioxidant compounds facilitate the reduction of metal ions to the nanoscale while simultaneously enhancing nano-particle stability and biocompatibility [7,8].

The medicinal plant *Withania coagulans*, which belongs to the Solanaceae family, is abundant in bioactive substances

such alkaloids, flavonoids and withanolides that help in the eco-friendly green synthesis of metal nanoparticles [9]. It was found that phenolic-capped AgNPs were a synthetic mono-dispersed nanoparticle that effectively controlled the virulence characteristics and biofilm development of bacteria that expressed carbapenemase [10,11]. AgNPs are synthesised using the leaf extract of *W. coagulans* reported as antioxidant and antibacterial against key pathogens such as *Salmonella typhi*, *Klebsiella pneumoniae* and *E. coli* [12-15]. Therefore, the current study was aim to assess the antibacterial efficacy of green produced AgNPs on carbapenem-resistant pathogen gene regulation using leaf extract of *W. cogulans.*

EXPERIMENTAL

Extraction of phytochemical: Fresh plant was collected and washed with distilled water then kept for drying under shade for several days until it was completely dried. The well dried leaves were crushed into fine powder using mixture grinder and sieved. About 10 g of leaf powder was extracted with 100 mL of different solvent in a Soxhlet apparatus for 6 h at 50 ºC.

Qualitative phytochemical analysis

Test for alkaloids: A 5 mL of HCl (1%) was mixed with 2 mL of extract and then filtered. From this 1 mL of sample was taken separately in a test tube and few drops of Hager's was added. Appearance of yellow precipitate designates the existence of alkaloids.

Test for saponins: A 10 mL of distilled water was mixed with 1 g of powdered crude extract and then boiled and filtered. Then 5 mL of filtrate was taken in a tube and shaken for 2 min. Appearance of foam after shaking designates the existence of saponins.

Shinoda's test for flavonoids: A 5 mL of ethanol and 500 mg of powdered dry extract were combined, boiled gently and then filtered. The filtrate was introduced with few pieces of magnesium chips and few drops of strong HCl was then added to the combination. Flavonoids are indicated by the presence of a pink, orange or red to purple colour.

Test for tannins: A 500 mg of powdered dry extract was added to 10 mL of distilled water, the mixture was then filtered and few drops of 1% alcoholic $FeCl_3$ solution are added to the filtrate. Occurrence of a blue-black, green or blue-green precipitate designates the existence of tannins.

Detection of terpenoids: A 10 mL of distilled water was mixed with 0.5 g of dried crude extract and dissolved under magnetic stirrer. The sample was then filtered and a few drops of 1% alcoholic $FeCl_3$ solution were added to the filtrate. Tannins are indicated by the presence of a blue-black precipitate.

Test for steroids: Equal volumes of acetic acid and chloroform were used to dissolve 100 mg of plant extracts. A few drops of strong sulfuric acid are added after the sample. The formation of a reddish-brown ring between acid and chloroform signifies the existence of a steroid.

Test for cardiac glycosides: Plant extracts were diluted with chloroform and let vapourize until they were completely dry. Additionally, 0.4 mL of glacial acetic acid with a trace amount of $FeCl_3$ was then added to sample and placed in a small test tube introduced carefully 0.5 mL of conc. H_2SO_4 by the side of the test tube, blue colour appears in the acetic acid layer suggesting that it contains of glycosides.

Detection of phenols: A few drops of $FeCl_3$ were added to 10 mL extract which results in the formation of a bluish-black colour confirming the presence of phenol.

Coumarins: In a test tube, 3 mL of 10% NaOH solution was mixed with 2 mL of plant extract. Formation of intense yellow colour indicating the presence of coumarins

Phylogeny analysis: The whole plant of *W. coagulans* was collected from Thiruvarangam, India and authenticated with the Botanist of Annamalai University. DNA isolation was carried out by taking 1 g of cleaned plant fresh leaf sample crushed in mortar and pestle using liquid nitrogen. A 2% cetyltrimethylaonium bromide (CTAB), 100 Tris- pH 8.0, 20 EDTA and 1.7 M NaCl with 0.3% (v/v) β-mercaptoethanol were used as a lysis buffer for isolation of total genomic DNA. The pellet obtained was suspended in 30 µL TE buffer. The quality of the isolated DNA was analysed on 0.8% agarose gel electrophoresis and the quantity was checked using a NanoDrop spectrophotometer. The extracted DNA was stored chilled at -20 ºC.

DNA amplification and sequence analysis: The reaction mixture of 25 µL contained 100 ng DNA templet, 0.5 U DreamTaq DNA Polymerase enzyme (Thermo Fischer), 10 dNTPs, 2.5 MgCl2, 10X DreamTaq Buffer and 0.5 µM rbcLa-F,5'-ATGTCACCACAAACAGAGACTAAA GC-3' and rbcLa-R, 5'-GTAAAATCAAGTCCA CCRCG-3' were amplified using standard procedure by initial activation at 95 ºC for approximately 10 min, followed by repeated cycling that included a denaturation phase at 95 ºC for about 45 s, an annealing phase at 58 ºC for roughly 45 s and an extension phase at 72 ºC for about 45 s. After completion of the cycling steps, the run concluded with a final extension period at 72 ºC lasting approximately 10 min. After cleaning all samples with the Qiagen Gel Extraction kit to get rid of excess primer dimers, templates and dNTP, the Sangers technique was used to sequence them [16]. The nucleotide sequences from *W. coagulans* have been compared to sequences contained in NCBI data-base and searched similarity with BLAST.

Green synthesis of AgNPs: Silver nanoparticles (AgNPs) were produced by combining an aqueous leaf extract of *W. coagulans* with 50 mM $AgNO_3$ solution at 1:9 ratio. This synthesis process, conducted at 40 ºC on a hot plate for 3 h. The reaction mixture from pale yellow to dark brown sample was subjected to UV Vis spectroscopy. Sample was centrifuged at 3000 rpm then supernatant was recentrifuged at 10,000 rpm for 15 min and the precipitates of AgNPs were washed three times with distilled water dried at 165 ºC. Dried samples calcined at 600 ºC to get fine powder. This powder was subsequently utilised for FT-IR spectra, SEM and TEM analysis.

Antibacterial activity: Various concentrations of AgNPs (100, 50 and 25 µg/mL) were tested against drug resistant pathogenic bacteria. In 20 mL NB, bacteria were grown for 24 h at 37 ºC with 120 rpm stirring and a standardised inoculum (1×10^8 CFU/mL) was prepared for each bacterial strain. All cultured bacteria incubate at 37 ºC for 24 h while shaking. Next, 100 µL of grown bacterial cell suspensions

spread on muller Hinton agar plates using sterile cotton swab. Different Ag-NPs concentrations were added to sterile disc and placed over the agar surface along with positive control imipenem and incubated at 37 ºC for 24 h. The bacterial strains' inhibitory zones were measured in by zone scale (Himedia) after 24 h [17].

Effect of AgNP on gene expression inhibition

Bacterial cell treatment: Bacterial cultures were maintained under standardised laboratory conditions until they reached the mid-logarithmic phase of growth, as measured by optical density studies. At this point, cultures were exposed to AgNPs at concentration of 20 µg/mL earlier established *via* preliminary susceptibility testing. Culture receiving only imipenem 30 µg/mL served as control. After being exposed to nanoparticle cultures were allowed to undergo transcriptional reactions for a 18 h at 37 ºC. Following incubation, bacterial cells from both treated and control groups were collected by centrifugation and washed pellet used for total RNA extraction (Himedia kit) to evaluate variations in $bla_{\text{NDM-1}}$ expression. Three replicates were kept and the data were analysed statistically.

RNA extraction and *c*DNA synthesis: Total RNA was extracted from phytochemical-treated and untreated bla_{NDM}-positive bacterial cultures using a coercial RNA purification system that included DNase treatment to eliminate genomic DNA (Himedia). RNA concentration and purity were assessed spectrophotometrically and integrity was confirmed by electrophoretic evaluation. Equal amounts of high-quality RNA from each sample were used for first-strand *c*DNA synthesis with a standard reverse transcription kit. No-reverse-transcription controls were included to ensure the absence of DNA contamination.

qRT-PCR analysis: The SYBR Green based detection chemistry was employed for quantitative real-time PCR (qRT-PCR). Gene-specific primers were used to amplify the carbapenemase gene $bla_{\text{NDM-1}}$, with 16S rRNA serving as endogenous reference control. For each biological assay, amplification reactions were performed in triplicate. Specific forward and reverse primers were used for both the house-keeping gene (16S rRNA) and the target gene and bla_{NDM}. Melt curve analysis and anticipated amplicon size confirmation were used to establish primer specificity. To verify the assay reliability, no-template and no-RT controls were incorporated throughout every run. Cycle threshold (Ct) values were automatically calculated by the instrument software. Relative expression of $bla_{\text{NDM-1}}$ in treated isolates compared with untreated controls was determined using the ΔΔCt method, with 16S rRNA serving as the housekeeping reference gene. Fold-change values were calculated as 2^(ΔΔCt) and only reactions showing consistent triplicate cycle threshold values and specific melt curves were included in the analysis.

Cytotoxicity studies: A cell viability test was used to check the cytotoxicity of the synthesised AgNPs by triplicate manner. The A549 cells were grown in 96-well plates at the density of 5×10^3 cells/well in the presence of 200 µL of DMEM with 10% FBS. After getting particular cell density, AgNPs (1 µg to 100 µg) were added along with fresh DMEM and incubated for 48 h. Then 10 µL of MTT (5 mg/mL) was added and the cells were incubated for 4 h at 37 ºC. The MTT solution was then disposed of and incubated in dark for 40 min after the addition of DMSO (100 µL). The absorbance was recorded at 570 nm using a scanning multi-well spectrophotometer [18].

RESULTS AND DISCUSSION

The formation of AgNPs using *Withania coagulans* extract was confirmed by UV-Visible spectrophotometry (Fig. 1). The spectra showed a prominent absorption band in the deep-UV region (≈ 210-230 nm), attributed to π→π* transitions of phenolic and flavonoid constituents present in the plant extract, which act as natural reducing and capping agents. A secondary broad peak observed between 300-360 nm corresponds to the surface plasmon resonance (SPR) characteristic of nanoscale Ag with polyphenols indicating successful reducing phytochmicals. The visible colour change of the reaction mixture from pale yellow to brown confirmed the formation of AgNPs. Following calcination, the yield of AgNPs was 3.22 g per 100 mL of reaction mixture. These findings are consistent with earlier reports showing that phytochemicals of *W. coagulans* effectively reduce and cap AgNPs, producing stable colloids with well-defined SPR signatures. Previous investigations on naturally and synthetically produced AgNPs have consistently reported identical SPR peaks around 360-370 nm, supporting particles synthesis, stability and nanoscale size distribution [19,20].

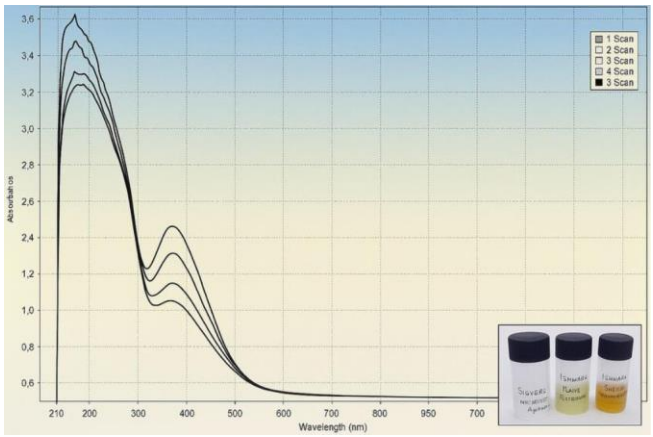

Fig. 1. UV-Visible spectrum of green synthesised silver nanoparticles

The FTIR spectrum (Fig. 2) displays several prominent absorption bands indicating the presence of phytochemical functional groups of silver nanoparticles synthesised using *W. coagulans* extract. A strong, broad peak around 3400 cm^{-1} corresponds to O–H stretching vibrations of alcohols suggesting phenol role as reducing agents [21]. Peaks observed near 2920-2850 cm^{-1} represent C–H stretching confirming the presence of terpenoids and other lipid-derived phytochemicals [22]. A distinct peak close to 1630 cm^{-1} indicates C=O stretching or amide-I vibration, commonly associated with proteins and withanolide structures, implying that these biomolecules act as capping and stabilizing agents for AgNPs. Additional peaks at 1450-1380 cm^{-1} can be attributed to C–N or C–C stretching [23] characteristics of alkaloids and phenolic com-

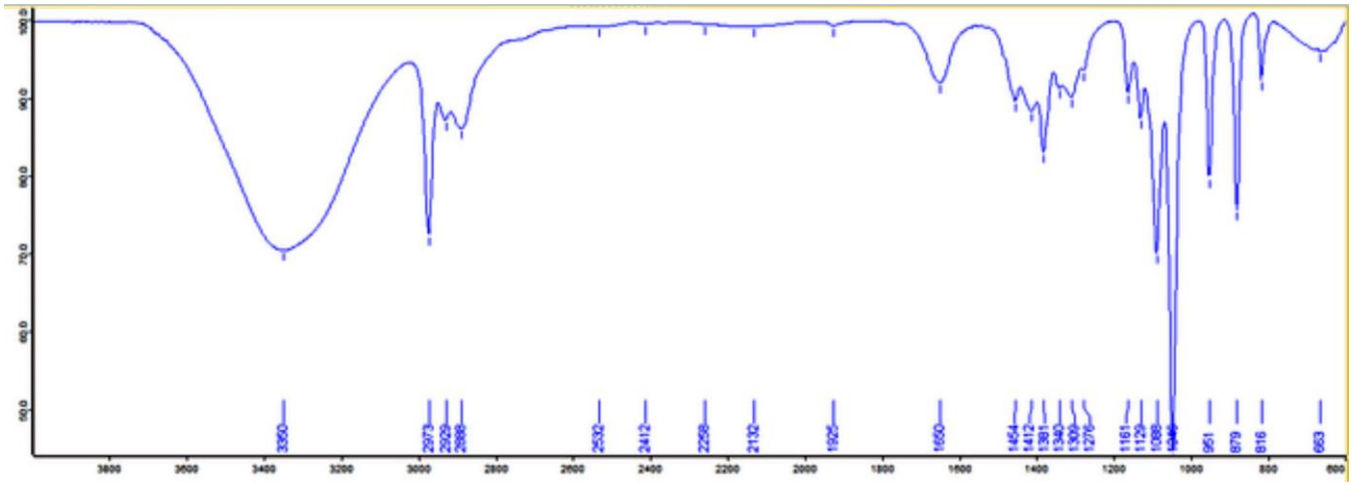

Fig. 2. FTIR spectrum or synthesised silver nanoparticles

pounds. Strong signals between 1100-1000 cm^{-1} correspond to C–O–C and C–O stretching, representing glycosides and polyols commonly found in *W. coagulans*. The absorption bands below 900 cm^{-1} suggest the presence of aromatic bending vibrations, confirming phytochemical diversity.

Morphology: The SEM micrographs of *W. coagulans* mediated AgNPs (Fig. 3a) were irregular aggregates approximately 80-95 nm. The presence of plant-derived biomolecules that function as reducing and capping agents causes mild agglomeration of nanoparticles, which is typical of biologically synthesised AgNPs. These surface-bound phytochemicals encourage particle clustering and aid in the stabilisation of nanoparticles. From the TEM micrograph, it is clear that the synthesis of AgNPs (Fig. 3b) with a spherical shape has been successful. The nanoparticles are well dispersed and not clumped together. They range in size from 10 to 50 nm, as indicated by the scale bar. The good dispersion and uniform electron density confirm the successful formation of crystalline AgNPs with a fairly uniform shape. These findings match previous research that has reported similar results in the biosynthesis of AgNPs [24].

Phylogenetic analysis: The pairwise evolutionary distances (Table-1) calculated using the maximum composite likelihood (MCL) method provide quantitative insight into the genetic divergence among the studied rbcL sequences. The plant shows the minimum evolutionary distances with *W. frutescens* (0.00589) and *W. somnifera* (0.01063), indicating high sequence similarity and close phylogenetic relatedness. A slightly higher but still low divergence (0.01660) was observed with *W. coagulans*, supporting the placement of the isolate within the *Withania* clade. In contrast, the isolate exhibits substantially greater distances from *Solanum corymbosum* (0.02939), *Nicotiana tabacum* (0.03800), *D. stramonium* (0.01421) and *D. metel* (0.03000). These higher values reflect increased evolutionary separation and are consistent with the branching pattern observed in the phylogenetic tree. The phylogeny based on the rbcL gene sequence clearly positions the isolate within the Solanaceae family, forming a strongly supported clade with members of the genus *Withania* (Fig. 4). Bootstrap values associated with these nodes (56-88%) provide moderate to strong support for this grouping, confirming the isolate's high similarity to known *Withania* taxa. A

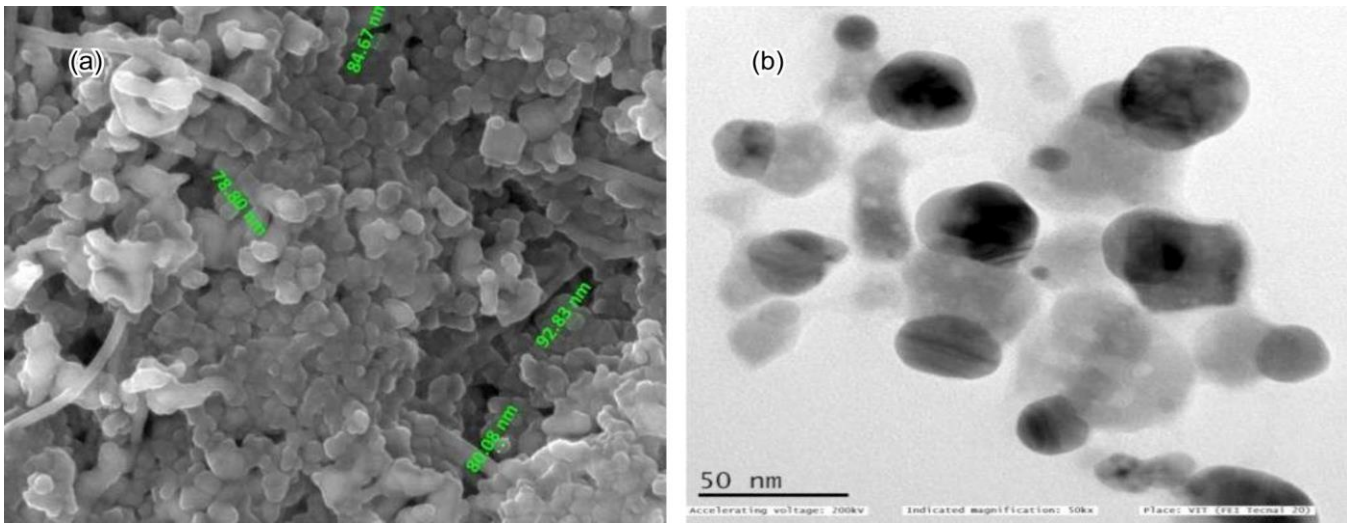

Fig. 3. (a) Scanning electron microscope image of green AgNPs with spherical nanoparticle and (b) TEM image of AgNPs with moderate dispersed spherical NPs

TABLE-1
PAIRWISE EVOLUTIONARY DISTANCES OF STUDY PLANT R5P GENE

Strains	Isolate	*W. frutescens*	*W. somnifera*	*D. stramonium*	*S. corymbosum*	*D. metel*	*N. tabacum*	*W. coagulans*
Isolate								
DQ368401.1 *Withania frutescens*	0							
DQ353862.1 *Withania somnifera*	0.005891	0.033797						
OM616889.1 *Datura stramonium*	0.010638	0.039058	0.011069					
PQ474775.1 *Solanum corymbosum*	0.014213	0.043006	0.013305	0.006572				
MH767728.1 *Datura metel*	1.001058	1.038344	1.029399	1.041286	1.037228			
KC825342.1 *Nicotiana tabacum*	0.016608	0.041943	0.014446	0.009087	0.009088	1.045783		
PX353023.1 *Withania coagulans*	0	0	0.005891	0.010638	0.014213	1.001058	0.016608	

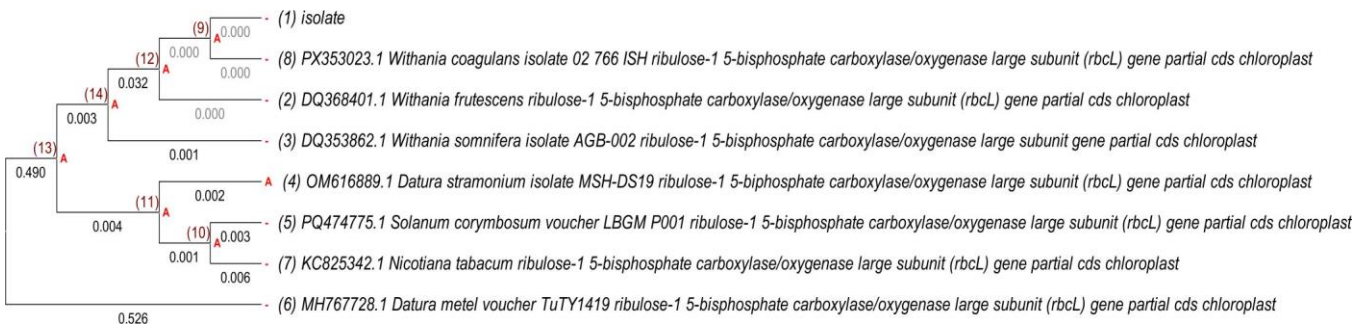

Fig. 4. Maximum-likelihood phylogenetic tree constructed using the rbcL gene sequences showing the evolutionary placement of the collected plant

distinct sister clade includes *D. stramonium* (OM616889.1) and *D. metel* (MH767728.1), separated by longer branch lengths (0.002-0.526), demonstrating greater evolutionary distance from the *Withania* cluster. Additional branching shows more distant relationships to *S. corymbosum* (PQ474775.1) and *N. tabacum* (KC825342.1), consistent with expected phylogenetic separation within Solanaceae. These taxa form deeper branches with longer evolutionary distances, supporting their divergence from both *Withania* and *Datura* lineages.

P**hytochemical screening:** Qualitative phytochemical screening of *W. coagulans* extracts prepared using solvents of differing polarity revealed marked variation in the distribution of secondary metabolites (Table-2). Highly polar solvents such as methanol and water yielded the greatest diversity of phytochemicals, whereas non-polar solvents such as hexane extracted fewer components. Methanol extract exhibited the strongest reaction for flavonoids, phenols, tannins, glycosides and coumarins than other solvents. This observation aligns with earlier reports demonstrating that methanol is highly efficient in extracting phenolic and flavonoid constituents from *W. coagulans* due to its polarity and solvation capacity. The chloroform extract showed high abundance of phenols, steroids, terpenoids and alkaloids reflecting the intermediate polarity of chloroform, which facilitates extraction of moderately lipophilic metabolites. Ethyl acetate extract showed moderate levels of phytochemical consistent with the solvent's semi-polar nature. In contrast, the hexane extract exhibited weak detection of most phytochemicals. Similar limited extraction profiles using hexane have been observed in studies on *Withania* species, where only sterols and triterpenes were efficiently recovered [25].

Water extract showed absence of tannins and glycosides and less significant intensity of other compounds reflecting the selective solubility of these compounds in hot aqueous conditions. The strong presence of phenolic and terpenoid constituents in polar extracts supports their known antioxidant and antimicrobial properties, as widely documented in *W. coagulans* phytochemistry [26]. Methanolic and chloroform extracts exhibited a higher diversity of bioactive compounds, indicating their effectiveness in extracting phenolics, alkaloids,

TABLE-2
QUALITATIVE PHYTOCHEMICAL EVALUATED UNDER DIFFERENT SOLVENTS

Phytochemical test	Hexane extract	Chloroform extract	Ethyl acetate extract	Methanol extract	Water extract
Alkaloids	+	++	+	++	+
Flavonoids	–	+	++	+++	+
Tannins	+	–	+	++	–
Saponins	–	–	–	–	–
Terpenoids	+	++	+	+	+
Phenols	+	+++	+	+++	+
Glycosides	–	+	+	++	–
Steroids	–	++	+	+	–
Coumarins	–	–	–	++	–

flavonoids and terpenoids. In contrast, hexane extracts showed limited recovery, primarily of sterols and triterpenes, consistent with previous reports on *Withania* species. Aqueous extracts lacked tannins and glycosides and showed weaker representation of other constituents, reflecting solvent-dependent selectivity. The predominance of phenolic and terpenoid compounds in polar extracts aligns with the reported antioxidant and antimicrobial potential of *W. coagulans*, supporting their suitability for further bioactivity-guided studies [27].

Antibacterial activity: The methanol extract of plant displayed broad-spectrum antimicrobial effects towards all tested pathogens, with inhibition zones expanding in a concentration dependent manner (Table-3). The extract showed the greatest effectiveness against all pathogens and maximum activity over *K. pneumoniae* (19-22 mm) and *S. pneumoniae* (22 mm) followed by *P. aeruginosa* 13-16 mm at 100 µg/mL. Most isolates showed moderate activity when the concentration was lowered to 50 µg/mL, especially *S. pneumoniae* (18 mm) and *Citrobacter koseri* (16 mm), suggesting reduced diffusion and moderate availability of bioactive components. The extract was most effective against *C. koseri* (13 mm), *Proteus vulgaris* (11 mm) and two *P. aeruginosa* (10-13 mm) at 25 µg/mL. However, other isolates did not exhibit detectable zones because of strain-specific resistance or phenotypic heterogeneity [28]. The methanolic extract of *W. coagulans* has been widely reported to inhibit a range of clinically relevant pathogens, including multidrug-resistant Gram-negative isolates [29].

TABLE-3
ANTIBACTERIAL ACTIVITY OF
METHANOL EXTRACT OF *W. coagulans*

Isolates	Pathogen tsted	25 µg	50 µg	100 µg
1	*Citrobacter koseri*	13	16	18
2	*Klebsiella pneumoniae 1*	–	16	22
3	*Proteus vulgaris 1*	11	13	15
4	*Klebsiella pneumoniae 2*	–	–	19
5	*Pseudomonas aeruginosa 1*	10	13	16
6	*Proteus vulgaris 2*	–	10	20
7	*Pseudomonas aeruginosa 2*	2	10	13
8	*Streptococcus pneumoniae*	–	18	22

The biosynthesised AgNPs demonstrated strong antibacterial activity against all tested clinical isolates, with inhibition zones increasing in a concentration-dependent manner. At 25 µg/mL, AgNPs produced inhibition zones ranging from 17-20 mm, indicating substantial baseline activity even at lower concentrations. Notably, *P. vulgaris* and *C. koseri* showed the highest susceptibility at this dose, each exhibiting 20 mm zones. At 50 µg/mL, inhibition remained consistently high across isolates mainly pathogens including *K. pneumoniae*, *P. vulgaris* and *P. aeruginosa* showing 18-20 mm zones (Table-4). A further increase to 100 µg/mL enhanced the inhibitory effect in nearly all isolates, producing zones of 20-21 mm, particularly in *K. pneumoniae*, *S. pneumoniae* and *C. koseri*. These results confirm that AgNPs efficacy increases with concentration and that Gram-negative isolates exhibit strong sensitivity, likely due to nanoparticle-mediated membrane disruption, protein inactivation and oxidative stress. The biosynthesised AgNPs exhibited strong broad-spectrum antibacterial activity, consistent with earlier studies demonstrating potent inhibition of both Gram-positive and Gram-negative pathogens [30]. AgNPs have electrostatic interactions with the negatively charged components found on the bacterial cell wall. There will be damage to the cell wall and membrane due to this electrostatic interaction; this results in cell lysis due to leakage of cellular materials. Different phytochemicals cap specific crystal facets of nanoparticles. Higher concentrations of flavonoids and polyphenols often result in smaller, spherical and more uniform nanoparticles with greater zeta potential helps to improve the colloidal stability and thus improve cellular permeability [31].

Effect of AgNPs on gene expression analysis: The quantitative evaluation of gene expression with and without AgNPs across all carbapenem-resistant isolates are given in Fig. 5. One-way ANOVA was used in the statistical analysis to compare the relative gene expression of the NP-treated and untreated groups. The mean ± SD of triplicate experiments is used to express the data. Statistical significance was defined as a p value of less than 0.05. Although the degree of down-regulation differed among isolates, fold-change values obtained from the 2^(ΔΔCt) technique showed consistent down-regulation in all samples (Table-5). *K. pneumoniae 1* (0.0451), *Citrobacter* sp. (0.0674) and *S. pneumoniae* (0.0545) showed the greatest gene down regulation suggesting that AgNPs had a very significant inhibitory effect on these strains. PA (0.0788), KP2 (0.2486) and PV2 (0.3110) showed significant down-regulation, while PA2 (0.5147) showed the less genetic regulation, indicating improved tolerance or decreased sensitivity toward nanoparticle. The isolates PV (0.3479) and KP2 (0.2486) showed intermediate gene expression reflecting variability in does response on nanoparticle treatment (Fig. 6). Before treatment, relative expression values ranged from 0.15 to 0.96, indicating normal baseline transcriptional activity

TABLE-4
ANTIBACTERIAL ACTIVITY OF *W. coagulans* MEDIATED AgNPs ON IPM RESISTANT CLINICAL PATHOGENS

Isolates code	Organisms	IPM	Negative control	25 µg	50 µg	100 µg
CK	*Citrobacter koseri*	< 5	–	18	20	20
KP1	*Klebsiella pneumoniae*	< 5	–	17	17	19
PV1	*Proteus vulgaris*	< 5	–	20	20	20
KP2	*Klebsiella pneumoniae*	8	–	19	19	21
PA1	*Pseudomonas aeruginosa*	< 5	–	17	18	18
PV2	*Proteus vulgaris*	< 10	–	20	20	20
PA2	*Pseudomonas aeruginosa*	< 8	–	18	18	19
SP	*Streptococcus pneumoniae*	< 5	–	19	20	21

TABLE-5
ANTIBACTERIAL ACTIVITY AMONG IPM RESISTANT CLINICAL PATHOGENS TREATED WITH *W. coagulans* MEDIATED AgNPs

Sample	Imipenem treated				AgNP treated				ΔΔCt	Fold change
	Treatment_Ct value	House keeping_Ct value	ΔCt	Relative expression	Treatment_Ct value	House keeping_Ct value	ΔCt	Relative expression		
CK	21.027	20.129	0.898	0.5366 ± 0.02	24.137	19.348	4.789	0.0361 ± 0.002	3.891	0.067 ± 0.0050
KP	19.621	19.363	0.258	0.8362 ± 0.02	22.559	17.832	4.727	0.037 ± 0.002	4.469	0.045 ± 0.0040
PV	19.434	19.379	0.055	0.9625 ± 0.02	22.98	21.402	1.578	0.33 ± 0.015	1.523	0.347 ± 0.0150
KP	20.043	18.723	1.32	0.4005 ± 0.02	22.793	19.465	3.328	0.09 ± 0.005	2.008	0.248 ± 0.010
PA	19.441	18.871	0.57	0.6736 ± 0.02	22.355	18.121	4.234	0.053 ± 0.003	3.664	0.078 ± 0.0050
PV	22.874	20.168	2.706	0.1532 ± 0.01	23.27	18.879	4.391	0.047 ± 0.002	1.685	0.311 ± 0.0150
PA	21.882	20.145	1.737	0.2999 ± 0.01	23.152	20.457	2.695	0.154 ± 0.007	0.958	0.514 ± 0.02
SP	21.527	21.027	0.5	0.7071 ± 0.015	23.27	18.574	4.696	0.0385 ± 0.02	4.196	0.0545 ± 0.005

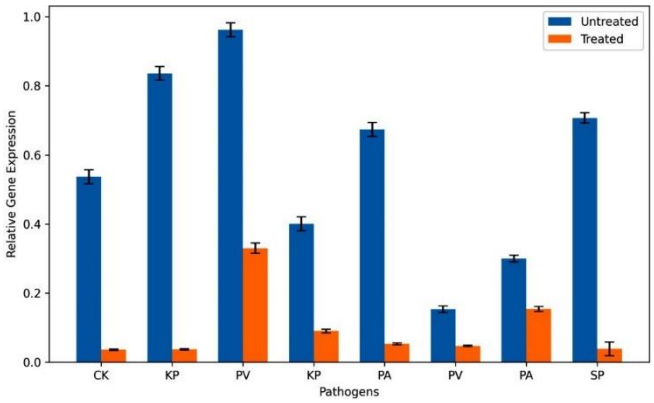

Fig. 5. Relative resistant gene expression levels among pathogens in AgNPs treated and untreated

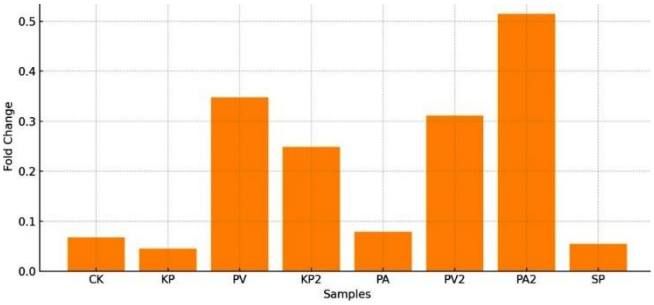

Fig. 6. Drug resistance gene expression fold changes among pathogens treated with AgNPs

within the carbapenem-resistant isolates. After AgNPs exposure, however, relative expression values dropped dramatically to 0.03-0.33, reflecting a substantial decline in mRNA abundance. This shift resulted in ΔΔCt values between approximately 1.5 and 4.7 cycles, translating into fold-change values between 0.04 and 0.51, which correspond to down-regulation of gene expression [21]. According to a recent research report [32], the selective advantage of carbapenemase expression may be diminished by the greater local drug concentration, which would attenuate transcriptional activation of resistance genes.

Gene expression analysis has proven to be an effective approach for screening potential antimicrobial agents. Reduced fold-change in RNA expression, corresponding to a 70–95% downregulation, confirms that AgNPs exert a strong inhibitory effect on the transcriptional activity of resistance-associated genes [32]. The magnitude of cycle threshold changes, although variable between isolates demonstrated reduced expression, suggesting a strain-dependent action of AgNPs. Even at lower concentrations, AgNPs have been demonstrated to produce intracellular ROS, which may be related to inhibition of transcriptional factors, pospharylation of kinase domain and down regulation of genes [32,33].

Cytotoxicity studies: The cytotoxicity results for biosynthesized AgNPs on A549 cells (1-100 μg/mL) showing very high viability even at 100 μg/mL are consistent with other reports indicating relatively low to moderate toxicity of AgNPs in similar systems. The lowest viability is 91.8% at 100 μg/mL, acceptable cytotoxicity was recorded between 1-50 μg/mL and slightly insignificant at 100 μg/mL (Table-6). The cytotoxicity analysis revealed that AgNPs exerted only mild toxicity toward A549 epithelial cells within the tested concentration range. Cell viability remained high, measuring 95% at 25 μg/mL, 93% at 50 μg/mL and 91.8% at 100 μg/mL, compared to 100% in the untreated control. Recently, AgNPs green synthesised AgNPs found to reduce cell viability in a dose-dependent way, with significant toxicity observed only at 100 μg/mL [34]. This indicates a slight, dose-dependent decline in viability, however, the overall reduction was minimal, showing that the nanoparticles did not significantly impair cell survival even at the highest concentration. Microscopic observation further supported these findings, as treated cells retained normal epithelial morphology with intact cell shape, adherence and density (Fig. 7). For instance, studies have documented membrane blebbing, chromatin condensation and nuclear fragmentation in treated A549 cells

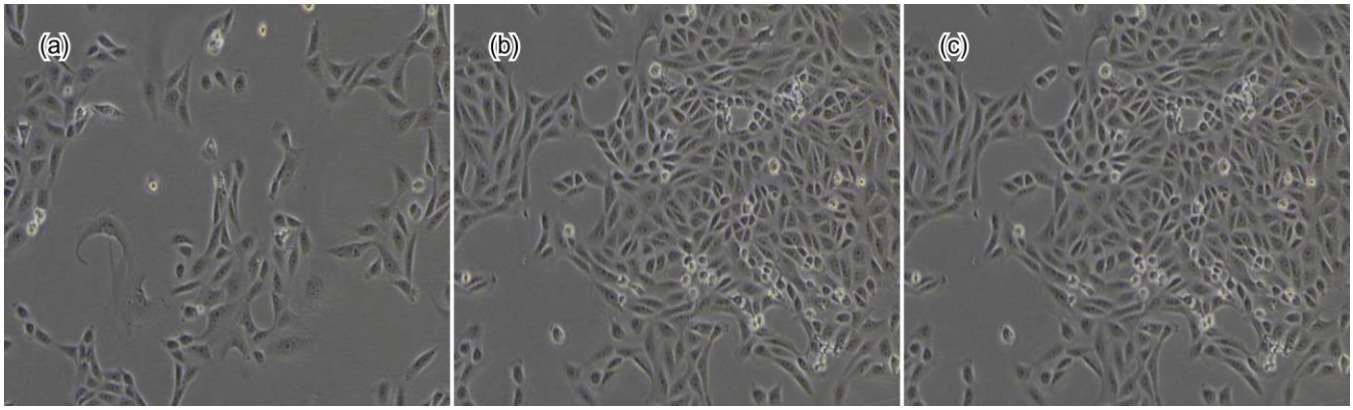

Fig. 7. Effect of AgNPs treatment on apoptosis in cells: untreated control (a), 50 mg AgNPs (b) and 100 mg AgNPs (c)

TABLE-6
CYTOTOXICITY EFFECT OF BIOSYNTHESISED AgNPs

Concentration (µg/mL)	Viability (%)
100	91.8 ± 0.015
75	92.6 ± 0.05
50	93 ± 0.01
25	95 ± 0.01
10	97.8 ± 0.02
5	99 ± 0.05
1	100 ± 0.05
0	100 ± 0.05

[35], compared to smooth, well-spread control cells. Furthermore, exposure to AgNPs can increase surface roughness and reduce cell height, as shown by atomic force microscopy, suggesting changes in cytoskeletal organisation and cell stiffness [36,37].

Conclusion

The present study demonstrates that *Withania coagulans* extracts effectively mediate the green synthesis of silver nanoparticles (AgNPs), producing stable, spherical nanoparticles with well-defined size distribution (10-50 nm) and characteristic surface plasmon resonance. Phytochemicals, particularly phenolics, flavonoids, terpenoids and proteins, play a dual role as natural reducing and capping agents, contributing to nanoparticle stability, uniformity and biological activity. Methanolic and chloroform extracts were identified as the most effective solvents for isolating bioactive metabolites, validating their antioxidant and antimicrobial potential. Both the plant extracts and biosynthesized AgNPs exhibited concentration-dependent, broad-spectrum antibacterial activity, with Gram-negative isolates demonstrating higher susceptibility, likely through membrane disruption, oxidative stress and protein inactivation. The quantitative gene expression analysis revealed significant downregulation (70-95%) of carbapenem-resistance genes (bla_{NDM-1}), highlighting the capacity of AgNPs to interfere with transcriptional mechanisms associated with antimicrobial resistance. Cytotoxicity assays confirmed minimal adverse effects on A549 epithelial cells, even at the highest tested concentrations, suggesting that the AgNPs are biocompatible and safe for further biomedical applications. These findings indicate that *W. coagulans*-mediated AgNPs combine potent antimicrobial efficacy with low cytotoxicity, supporting their potential as sustainable, plant-based nanotherapeutics against multidrug-resistant pathogens.

ACKNOWLEDGEMENTS

The authors gratefully acknowledge Annamalai University, Chidambaram, Tamil Nadu, India (608002), for providing the necessary laboratory facilities, technical support and research environment to carry out this study.

CONFLICT OF INTEREST

The authors declare that there is no conflict of interests regarding the publication of this article.

DECLARATION OF AI-ASSISTED TECHNOLOGIES

During the preparation of this manuscript, the authors used an AI-assisted tool(s) to improve the language. The authors reviewed and edited the content and take full responsibility for the published work.

REFERENCES

1. R. Cantón, J.P. Horcajada, A. Oliver, P. Ruiz-Garbajosa and J. Vila, *Enferm. Infecc. Microbiol. Clin.*, **41**, 3 (2013); https://doi.org/10.1016/S0213-005X(13)70126-5
2. O. Caliskan-Aydogan and E.C. Alocilja, *Microorganisms*, **11**, 1491 (2023); https://doi.org/10.3390/microorganisms11061491
3. W.Y. Jamal, M.J. Albert and V.O. Rotimi, *PLoS One*, **11**, e0152638 (2016); https://doi.org/10.1371/journal.pone.0152638
4. E. Tacconelli, E. Carrara, A. Savoldi, S. Harbarth, S. Mendelson, P. Monnet, A. Pulcini, G. Kahlmeter, S. Borgel, C. Cauda, R. Coenen, A. Ouakrim, D. Voss, A. Dryden, M. Maher, C. Gasser and R. Hansen, *Lancet Infect. Dis.*, **18**, 318 (2018); https://doi.org/10.1016/S1473-3099(17)30753-3
5. S.H. Haji, F.A. Ali and S.T.H. Aka, *Sci. Rep.*, **12**, 15254 (2022); https://doi.org/10.1038/s41598-022-19698-0
6. S.M. Mousavi, S.M.A. Mousavi, M. Moeinizadeh, M. Aghajanidelavar, S. Rajabi and M. Mirshekar, *J. Basic Microbiol.*, **63**, 632 (2023); https://doi.org/10.1002/jobm.202200612
7. L. Castillo-Henríquez, K. Alfaro-Aguilar, J. Ugalde-Álvarez, L. Vega-Fernández, G.M. de Oca-Vásquez and J.R. Vega-Baudrit, *Nanomaterials*, **10**, 1763 (2020); https://doi.org/10.3390/nano10091763
8. S.A. Akintelu, Y. Bo and A.S. Folorunso, *J. Chem.*, **2020**, 3189043 (2020); https://doi.org/10.1155/2020/3189043

9. S. Qasim, A. Zafar, M.S. Saif, Z. Ali, M. Nazar, M. Waqas, A.U. Haq, T. Tariq, S.G. Hassan, F. Iqbal, X.G. Shu and M. Hasan, *J. Photochem. Photobiol. B*, **204**, 111784 (2020); https://doi.org/10.1016/j.jphotobiol.2020.111784
10. D. Tripathi, A. Modi, G. Narayan and S.P. Rai, *Mater. Sci. Eng. C*, **100**, 152 (2019); https://doi.org/10.1016/j.msec.2019.02.113
11. S.H. Zehra, K. Ramzan, J. Viskelis, P. Viskelis and A. Balciunaitiene, *Nanomaterials*, **15**, 252 (2025); https://doi.org/10.3390/nano15040252
12. F. Iftikhar, R. Qureshi, A. Siddiqa, K. Anwar, F. Arshad and Z. Mashwani, *Czech J. Food Sci.*, **42**, 192 (2024); https://doi.org/10.17221/39/2024-CJFS
13. X. Kuang, Y. Li, J. Zhu, W. Li and Z. Zhou, *Front. Chem. Eng.*, **4**, 941240 (2022); https://doi.org/10.3389/fceng.2022.941240
14. S. Scandorieiro, F.M.M.B. Teixeira, M.C.L. Nogueira, L.A. Panagio, A.G. Oliveira, N. Durán, G. Nakazato and R.K.T. Kobayashi, *Antibiotics*, **12**, 756 (2023); https://doi.org/10.3390/antibiotics12040756
15. D. Jini, S. Sharmila, A. Anitha, M.P. Pandian, P.D. Devi and S.R. Senthilkumar, *Sci. Rep*., **12**, 22109 (2022); https://doi.org/10.1038/s41598-022-24818-x
16. N.B. Bare, P.S. Jadhav and M. Ponnuchamy, *J. Appl. Biol. Biotechnol*., **12**, 69 (2024); https://doi.org/10.7324/JABB.2023.145330
17. Q.U.A. Ahmad, F. Shafique, N. Afzal, I. Perveen, N. Koser, T.M. Dawoud, S. Alajmi, M. Alshahrani and H. Ali, *Chem. Biodivers.*, **22**, e202402839 (2025); https://doi.org/10.1002/cbdv.202402839
18. M. Rai, A. Yadav and A. Gade, *Biotechnol. Adv*., **27**, 76 (2009); https://doi.org/10.1016/j.biotechadv.2008.09.002
19. O. Gemishev, M. Panayotova, G. Gicheva and N. Mintcheva, *Materials*, **15**, 481 (2022); https://doi.org/10.3390/ma15020481
20. H.O. Khalifa, A. Oreiby, T. Mohammed, M.A.A. Abdelhamid, E.N. Sholkamy, S. Alqarni and A. Alshahrani, *Front. Cell. Infect. Microbiol*., **15**, 1599113 (2025); https://doi.org/10.3389/fcimb.2025.1599113
21. V. Ravichandran, S. Vasanthi, S. Shalini, M. Balakrishnan and R. Kumar, *Results Phys*., **15**, 102565 (2019); https://doi.org/10.1016/j.rinp.2019.102565
22. V. Pareek, S. Devineau, S.K. Sivasankaran, A. Bhargava, J. Panwar, S. Srikumar and S. Fanning, Front. Microbiol., 12, 638640 (2021); https://doi.org/10.3389/fmicb.2021.638640
23. S.P. Dubey, M. Lahtinen and M. Sillanpää, *Colloids Surf. A*, **364**, 34 (2010); https://doi.org/10.1016/j.colsurfa.2010.04.023
24. M. Ramzan, M.A.H.A. Abusalah, N. Ahmed, C.Y. Yean and B. Zeshan, *Int. J. Nanomed*., **19**, 13319 (2024); https://doi.org/10.2147/IJN.S475656
25. P. Raghav, N. Sharma, P. Choudhary, N. Kumar, R. Sharma, H. Badoni, R. Singh, S. Mehta and R. Joshi, Plant Sci. Today, 12, 1 (2025); https://doi.org/10.14719/pst.3288
26. M.M. Khalil, E.H. Ismail, K.Z. El-Baghdady and D. Mohamed, *Arab. J. Chem*., **7**, 1131 (2014); https://doi.org/10.1016/j.arabjc.2013.04.007
27. A. Khan, T. Younis, M. Anas, M. Ali, Z.K. Shinwari, A.T. Khalil, R. Ahmad and S. Iqbal, *BMC Plant Biol*., **25**, 574 (2025); https://doi.org/10.1186/s12870-025-06533-7
28. M.F. Baran, C. Keskin, A. Baran, A. Hatipoğlu, M. Yildiztekin, S. Küçükaydin, B. Demir and F. Akpinar, *Molecules*, **28**, 2310 (2023); https://doi.org/10.3390/molecules28052310
29. M.I. Khan, M. Maqsood, R.A. Saeed, A. Alam, A. Sahar and M. Kieliszek, *Molecules*, **26**, 6881 (2021); https://doi.org/10.3390/molecules26226881
30. F. Rodríguez-Félix, N. Ramírez-Beltrán, D. González-Mendoza, M. Hernández-Rodríguez and J. Torres, *J. Nanomater*., **2022**, 8874003 (2022); https://doi.org/10.1155/2022/8874003
31. M. Muhamad, N.A. Rahim, W.A.W. Omar and N.N.S.N.M. Kamal, *Bioinorg. Chem. Appl*., **2022**, 8546079 (2022); https://doi.org/10.1155/2022/8546079
32. F.A. Ebrahimi, E. Siasi, F. Yazdian, M. Ghorbani and S. Kiani, *Sci. Rep.*, **15**, 37708 (2025); https://doi.org/10.1038/s41598-025-21606-1
33. V.A. Kumar, T. Uchida, T. Mizuki, M. Kobayashi and S. Watanabe, *Adv. Nat. Sci.: Nanosci. Nanotechnol.*, **7**, 015002 (2016); https://doi.org/10.1088/2043-6254/7/1/015002
34. L. Xu, T. Takemura, M. Xu and N. Hanagata, *Microelectron. Expr.*, **1**, 74 (2011); https://doi.org/10.1166/mex.2011.1010
35. N. Alam, M. Hossain, M.A. Mottalib, S.A. Sulaiman, S.H. Gan and M.I. Khalil, *BMC Complement. Altern. Med*., **12**, 175 (2012); https://doi.org/10.1186/1472-6882-12-175
36. A. Hassan and H. Ullah, *J. Chem*., **2019**, 5264943 (2019); https://doi.org/10.1155/2019/5264943
37. N. Aati, J. Al-Qahtani, A. Al-Taweel, F. Al-Asmari, M. Al-Saleh and S. Al-Amri, *Front. Pharmacol*., **16**, 1653711 (2025); https://doi.org/10.3389/fphar.2025.1653711